Mon. Not. R. Astron. Soc. **000**, 000–000 (0000) Printed 12 April 1999 (MN LaTeX style file v1.4)

# Diffuse X-ray Emission from Late-Type Galaxy Haloes

A. J. Benson[1,3], R. G. Bower[1,4], C. S. Frenk[1,5] and S. D. M. White[2,6]

*1. Physics Department, University of Durham, South Road, Science Laboratories, Durham DH1 3LE, England.*
*2. Max Plank Institute für Astrophysik, Karl-Schwarzchild Strasse 1, D-85740, Garching, Germany.*
*3. E-mail: A.J.Benson@dur.ac.uk*
*4. E-mail: R.G.Bower@dur.ac.uk*
*5. E-mail: C.S.Frenk@dur.ac.uk*
*6. E-mail: swhite@mpa-garching.mpg.de*

12 April 1999



**ABSTRACT**

Current theories of galaxy formation predict that spiral galaxies are embedded in a reservoir of hot gas. This gas is able to cool onto the galaxy replenishing cold gas that is consumed in star formation. Estimates of the X-ray luminosity emitted in the cooling region suggest a bolometric luminosity of order $10 \times 10^{41}$ ergs s$^{-1}$. We have used ROSAT PSPC data to search for extended X-ray emission from the haloes of three nearby, massive, late-type galaxies: NGC 2841, NGC 4594 and NGC 5529. We infer 95% upper limits on the bolometric X-ray luminosities of the haloes of NGC 2841, NGC 4594 and NGC 5529 of 0.4, 1.2 and 3.8 $\times 10^{41}$ ergs s$^{-1}$ respectively. Thus the true luminosity lies well below the straightforward theoretical prediction. We discuss this discrepancy and suggest a number of ways in which the theoretical model can be brought into agreement with the observational results. A possible solution is that the gravitational potentials of these galaxies' dark matter haloes are weaker than assumed in the current model. Alternatively, the present day accretion may be substantially less than is required on average to build the disk over the Hubble time. Our results are, however, based on only three galaxies, none of which is ideal for this kind of study. A larger data set is required to explore this important problem further.

**Key words:** cooling flows - X-rays: galaxies - galaxies: formation - galaxies: NGC 2841, NGC 4594, NGC 5529

## 1 INTRODUCTION

In models of galaxy formation by hierarchical clustering, the disks of spiral galaxies form by the late accretion of gas cooling from an extended reservoir present around the galaxy. At the halo virial temperature, the dominant cooling mechanism is X-ray Bremsstrahlung. If the cooling rate is significant, this flux may be visible as a component of diffuse X-ray emission extending well beyond the galaxy's optical radius. In this paper, we set out to test the existence of a reservoir of cooling gas around three large, late-type galaxies, NGC 2841, NGC 4594 and NGC 5529.

If we assume that the mass of the present disk has been built up by a constant rate of accretion over the age of the universe ($t_0$), a simple estimate of the X-ray luminosity can be made from the binding energy of the disk.

$$L_X \approx \frac{\frac{1}{2} M_{\rm disk} v_{\rm esc}^2}{t_0} \qquad (1)$$

where $M_{\rm disk}$ is the present mass of the disk, $v_{\rm esc} = V_{\rm c}\left[2\ln(r_{\rm vir}/r_{\rm disk})+2\right]^{1/2}$ is the velocity required by material at the edge of the disk to escape the halo (assuming a flat rotation curve) and $V_{\rm c}$ is the measured circular velocity of the disk. Adopting parameters suitable for a large spiral galaxy such as NGC 2841 (ie., $M_{\rm disk} = 5\times10^{10} M_\odot$, and $V_{\rm c} = 317\,{\rm km/s}$), this suggests that the halo should emit a bolometric luminosity of $\sim 8\times10^{41}$ ergs s$^{-1}$. The picture of hierarchical galaxy formation developed by White & Frenk (1991, WF91; see also Kauffmann et al. 1993, Cole et al., 1994) predicts halo X-ray luminosities more directly by computing the cooling rate of gas as a function of time. At the present epoch, this model predicts an X-ray luminosity of $10\times10^{41}$ ergs s$^{-1}$ for galaxies like NGC 2841 (assuming that $\Omega_{\rm b}h^2 = 0.015$).

Previous studies of X-ray emission from nearby galaxies (e.g. Read, Ponman & Strickland, 1997) have concentrated on X-ray emission on scales comparable to the optical image of the galaxy. While extended emission has been detected in some groups of galaxies (e.g. Mulchaey et al. 1996, Trinchieri, Kim & Fabbiano 1994, Trinchieri, Fabbiano & Kim 1997), this emission is thought to be associated with the group potential. Our aim here is to test for the equivalent emission in *isolated* spiral galaxies. A few studies have

**Table 1.** Observed properties of the galaxies.

| Name | Heliocentric radial velocity (km/s)[a] | Distance (Mpc) | $W_{20}$ (km s$^{-1}$)[d] | $N_H$ ($10^{20}$ cm$^{-2}$)[e] | $r_{optical}$ (arcmin)[d] | $M_B$ | Hubble type |
|---|---|---|---|---|---|---|---|
| NGC 2841 | $638 \pm 3.0$ | $13.8 \pm 5.2$[b] | $674 \pm 4$ | 1.45 | $4.1 \pm 0.04$ | $-20.6 \pm 0.2$ | Sb |
| NGC 4594 | $1091 \pm 5.1$ | $24.54 \pm 2.5$[c] | $753 \pm 7$ | 3.67 | $4.4 \pm 0.04$ | $-23.0 \pm 0.2$ | Sa |
| NGC 5529 | $2885 \pm 5.1$ | $57.72 \pm 2.5$[c] | $592 \pm 5$ | 1.09 | $3.3 \pm 0.07$ | $-21.1 \pm 0.2$ | Sc |

[a] From the NASA Extragalactic Database (NED).
[b] de Vaucoulers (1979)
[c] From heliocentric radial velocity plus peculiar velocity correction assuming $H_0 = 50$ km s$^{-1}$ Mpc$^{-1}$.
[d] From the RC3 catalogue (available from NED), corrected for inclination.
[e] Dickey & Lockman (1990).

reported diffuse emission from isolated elliptical galaxies. However, this has been interpreted either as resulting from the expulsion of gas from the galaxy (e.g. Read & Ponman 1998, Mathews & Brighenti 1998) or as a relic of a collapsed group (Ponman et al. 1994). If diffuse X-ray emission from gas in the haloes of isolated galaxies proves undetectable, this need not imply that the mass of halo gas is small since the gas may simply be too diffuse to emit X-rays efficiently. However, it would then be unable to cool and would not flow to the centre of the halo. The goal of this paper is thus to test whether the gaseous disks of spiral galaxies are being built up by the accretion of halo gas at the present day. The alternative is that the gaseous disks of spiral galaxies were assembled at higher redshift and evolved essentially as closed systems thereafter.

The structure of this paper is as follows. In §2, we present the observational evidence for large-scale diffuse emission from spiral galaxies. We are not able to make any convincing detection; however, the upper limits to the luminosities that we find are almost an order of magnitude below the predictions of the WF91 model. In §3 we discuss the uncertainties in the models and describe how they might be modified to agree with the data. The prospects for future investigations are outlined in §4.

## 2 OBSERVATIONS

### 2.1 Target Selection

The primary aim of this paper is to test for the existence of diffuse X-ray emission from nearby isolated spiral galaxies. The galaxy must be nearby for the signal to be detectable. Furthermore, the galaxy must have a high circular velocity in order that the energy released by the cooling gas be large. A high circular velocity also aids detection by increasing the characteristic temperature of the emission so that less of the flux is absorbed by the neutral hydrogen in the Milky Way.

We created a suitable target list by searching for all spiral galaxies with recession velocities below 3000 km s$^{-1}$ and with HI 20% line widths greater than 580 km s$^{-1}$. Of the sixteen galaxies satisfying these criteria three have been observed by the ROSAT PSPC: NGC 2841, NGC 4594 (the Sombrero galaxy) and NGC 5529. The PSPC data for these fields were obtained from the Leicester Database and Archive Service (LEDAS).

**Table 2.** Measured rotation velocity and predicted gas temperature for the galaxies in our sample.

| Name | $V_c$ (km s$^{-1}$)[a] | $T_{vir}$ (keV)[b] |
|---|---|---|
| NGC 2841 | $317 \pm 2$ | $0.287 \pm 0.004$ |
| NGC 4594 | $358 \pm 4$ | $0.366 \pm 0.009$ |
| NGC 5529 | $277 \pm 3$ | $0.219 \pm 0.005$ |

[a] Calculated from HI line widths using the expression given in Tully & Fouqué (1985)
[b] As defined by White & Frenk (1991)

- NGC 2841. The Sb galaxy NGC 2841 is the nearest of our target galaxies. It has a flat rotation curve extending to the limit of HI observations, and is an archetype of galaxies with massive dark matter haloes (Kent, 1987). Its star formation properties have been studied extensively by Young et al. (1996) using both $H\alpha$ and far infra-red indicators.
- NGC 4594. Also known as M104 or the "Sombrero Galaxy," this is a highly luminous Sa seen almost edge on. Since this galaxy is bulge dominated, diffuse X-ray emission similar to that seen around E or S0 galaxies (Forman, Jones & Tucker 1985) might be expected. However, X-ray observations by the *Einstein* satellite revealed spectral properties and core X-ray colours typical of spiral galaxies (Kim, Fabbiano & Trinchieri 1992).
- NGC 5529. This is an Sc galaxy seen almost edge-on. Because of its relatively large distance and large isophotal diameter, this galaxy is likely to provide weaker constraints than the previous two.

Distances, line widths, optical radii, and other relevant properties of these galaxies are listed in Table 1. The distances to two of them (NGC 4594 and NGC 5529) had to be determined from their observed heliocentric radial velocity; a model of the local peculiar velocity field (Branchini et al. 1999) was used to correct the observed velocity to the true Hubble velocity using an iterative procedure. Table 2 lists the circular velocity of each galaxy as calculated from its HI line-width and also the virial temperature of the halo estimated in WF91.

### 2.2 Data Reduction

Ideally, we would like to compare the X-ray flux from an annulus centered on the galaxy (but excluding the optically bright region to avoid contamination from galactic emission) with similar annuli with centres on blank fields. This is not possible, however, because different ROSAT fields have different particle backgrounds. We have therefore adopted the procedure of first subtracting the detected events from a large radius annulus in the outer part of the PSPC detector as described in Snowden et al. (1994). Background corrected 'on source' and 'off source' fields may then be compared to determine the flux from the diffuse halo of the target galaxies. It is important to note that the background subtraction algorithm of Snowden et al. tends to produce negative flux in the off-source images because of the different point-source detection thresholds in the centre and outer parts of the ROSAT field. Our analysis takes this effect into account.

The analysis of the data was carried out using the Asterix package. The procedure for analysing each image was as follows. Firstly, point sources were detected down to a $3\sigma$ threshold and excluded by cutting out a circle centred on each source. The radius of this circle was set equal to the radius of the PSF enclosing 95% of the energy at the position of each source. For each image a background annulus of inner radius $0.5°$ and outer radius $0.7°$ was then used to estimate the vignetting corrected background count-rate, and to create two background-subtracted spectra from source-centred annuli with inner radius of 5 arcminutes and outer radii of 9 and 18 arcminutes. Choosing a fixed angular radius ensures that the blank field analysis is the same for each image. The outer radius was chosen to include the entire inner ring of the PSPC. This is comparable to the X-ray emitting region of the closer of our target galaxies (see §3). The $9'$ ring is matched to the X-ray emitting region of the more distant galaxy NGC 5529. The innermost aperture was excluded from the analysis in order to avoid contamination by the diffuse and unresolved stellar X-ray emission of the galaxy itself (cf. Read, et al. 1997, for example). The X-ray image of each galaxy is compared with the optical image in Figure 1.

The resulting spectra were analysed using the XSpec package. Within XSpec a model fit to each spectrum was obtained. The *mekal* X-ray emission and *wabs* absorption models were used. For each halo we adopted a virial temperature of 0.2keV. This is slightly below the virial temperatures estimated in Table 2, in order to obtain conservative estimates of the bolometric luminosity. The hot halo gas is assumed to have a metallicity of $0.3Z_\odot$ (where $Z_\odot$ is the Solar metallicity). Neutral absorption column densities varied between the fields and were taken from Dickey & Lockman (1990). The only remaining free parameter in these models is the overall normalization. This procedure appropriately weights the contributions of the different energy channels and corrects for the different neutral hydrogen cross-sections of the fields.

The fitted spectrum is then used to calculate the absorption corrected flux from each halo. These fluxes, shown in Table 4, are within the range 0.2 to 2.0 keV in order to minimise dependence on the assumed temperature. These are converted to pseudo-bolometric luminosities (0.001 to 10.0 keV) using the conservative temperature of 0.2 keV and the distances given in Table 1.

**Table 3.** The total counts per second in six blank fields. Background and point sources were removed in each case and an annulus from 5 to 9 arcminutes (ring 1) and from 5 to 18 arcminutes (ring 2) was selected.

| Field | Ring1 | Ring 2 |
|---|---|---|
| rp201558 | $-0.017 \pm 0.007$ | $-0.063 \pm 0.015$ |
| rp700255 | $-0.004 \pm 0.006$ | $-0.040 \pm 0.013$ |
| rp700319 | $-0.021 \pm 0.005$ | $-0.024 \pm 0.011$ |
| rp700376 | $-0.007 \pm 0.005$ | $-0.003 \pm 0.011$ |
| rp700387 | $+0.007 \pm 0.004$ | $-0.013 \pm 0.008$ |
| rp700389 | $-0.005 \pm 0.006$ | $-0.023 \pm 0.013$ |

For comparison, six off-source fields (Table 3) with point source targets were selected at random from the RIXOS survey (Mason et al 1998). As we have previously noted, the analysis procedure tends to produce a small negative count-rate when applied to the off-source fields. This is due (at least in part) to the different flux limits at which point sources are removed from the target and background annuli. The mean luminosity deficit in the off-source fields was added to the measured luminosities of the target galaxies. We investigated performing the analysis by subtracting the off-source and on-source count-rates and found that this procedure gives the same results to within 10%. Since the offset varies from field to field it is possible that our target fields have actual offsets somewhat different from the mean offset of our blank fields. We therefore measure the variance in the blank field offset and add this quantity in quadrature to the errors on the fluxes measured in our target fields. The variations from field to field are our dominant source of uncertainty.

The luminosities of the target galaxies are presented in Table 4. For each galaxy we expect a luminosity around $10 \times 10^{41}$ ergs s$^{-1}$. However none of the galaxies is detected at a $3\sigma$ confidence level in either of the annuli considered. Instead, our data sets 95% upper confidence limits of 0.37, 1.2 and $3.8 \times 10^{41}$ ergs s$^{-1}$ in the larger aperture for NGC 2841, 4594 and 5529 respectively. For NGC 5529, the relatively weak upper limit is due to the galaxy's larger distance. For the two more nearby galaxies, the upper limit lies an order of magnitude below the initial theoretical prediction.

### 2.3 Uncertainties in the Observations

In §3, we consider possible modifications to the model of WF91 that might alleviate the discrepancy with our data. First, we take a closer look at the assumptions we made in interpreting the observational data. There are a number of uncertain quantities that could affect our conclusions. Throughout the analysis we have consistently assumed conservative values for these quantities (i.e. those that would minimize the conflict between model and data.) It is nevertheless instructive to consider how these choices might affect our results.

The dominant source of uncertainty in our analysis is the process of background subtraction. Although an accurate estimation of the background from a mosaic of sur-

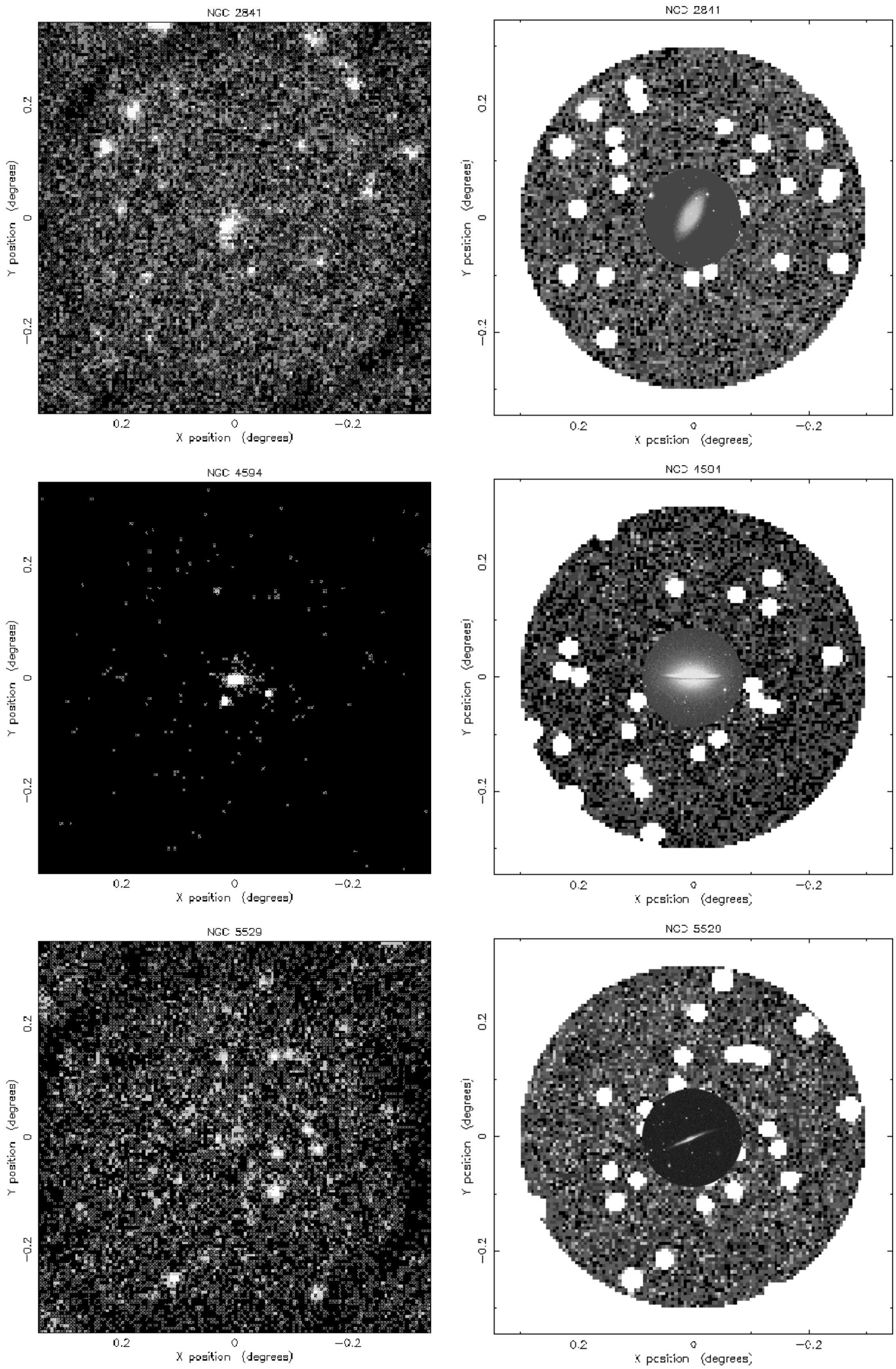


**Figure 1.** Source images for each galaxy in the sample. The left hand column shows the raw image and the right hand column the image after background subtraction, point source removal and selection of the region from 5 to 18 arcminutes. An optical image of each galaxy is superimposed on the X-ray image to give an appreciation of the size of the halo region.

**Table 4.** X-ray fluxes and bolometric luminosities for the haloes of three spiral galaxies. The fluxes and luminosities are determined for two annuli, with inner radius of 5 arcminutes and outer radii of 9 (ring 1) and 18 (ring 2) arcminutes. The first column gives the name of the galaxy. The flux corrected for blank field offsets is given in the following two columns, and the final two columns list the bolometric luminosity of each halo corrected for blank field offsets.

| **Galaxy** | **Bg. Corr. Flux (ring 1)** ($10^{-14}$ ergs/cm$^2$/s) | **Bg. Corr. Flux (ring 2)** ($10^{-14}$ ergs/cm$^2$/s) | **Bolometric** $L_X$ **(ring 1)** ($10^{41}$ ergs/s) | **Bolometric** $L_X$ **(ring2)** ($10^{41}$ ergs/s) |
|---|---|---|---|---|
| NGC 2841 | $5.62 \pm 10.33$ | $22.90 \pm 19.87$ | $0.03 \pm 0.06$ | $0.16 \pm 0.13$ |
| NGC 4594 | $17.96 \pm 11.33$ | $14.21 \pm 22.40$ | $0.44 \pm 0.28$ | $0.34 \pm 0.54$ |
| NGC 5529 | $5.91 \pm 10.03$ | $-2.28 \pm 19.22$ | $0.78 \pm 1.34$ | $-0.29 \pm 2.48$ |

rounding pointings would be preferable, our off-source fields indicate the magnitude of the uncertainty. Even using the 'worst case' field (rp201558), the predicted and observed count-rates still disagree by a factor of 2–3. Of course, it will always be impossible to eliminate the possibility that the X-ray emission from the target falls in an under-luminous region of the X-ray background.

Another important source of uncertainty is the extrapolation from ROSAT count-rate to bolometric flux. At the low temperatures appropriate to galactic halo gas, neutral hydrogen absorption in our own Galaxy has a strong effect. If our adopted values for the neutral hydrogen column density were inaccurate, this could have a substantial effect on our results. However these galaxies are at high Galactic latitude and we find that increasing the assumed column density by a factor of 3 over the values given by Dickey & Lockman (1990) only changes the inferred bolometric luminosity by 40%.

The effects of background correction and absorption alone cannot reconcile the observed and predicted luminosities. Altering the assumed temperature of the halo plasma, however, is a more promising alternative. This sensitivity arises because, at the relevant temperatures, most of the emission lies outside the 0.2–2.0 keV band of the observations, forcing us to extrapolate the model fit to lower energies. For example, at a temperature of 0.2 keV, 23% of the bolometric luminosity is emitted in the ROSAT 0.2–2.0 keV band, while at 0.1 keV, only 7% of the emission lies in this band. At even lower temperatures, the effect becomes even more pronounced. Applying a lower temperature model to the observed spectra, we find that a decrease in temperature by a factor of 4.0 (for NGC 2841) to 4.5 (for NGC 4594) is required to bring the observations into line with the predicted luminosity. It is not clear, however, how these lower temperatures can be accommodated within the theoretical model. We now turn to a detailed examination of this model.

## 3 DISCUSSION

The model presented by WF91 predicts that the X-ray luminosity due to gas cooling within a dark matter halo should be:

$$L_X = \dot{M}_{\rm cool}(r_{\rm cool}) V_c^2 \ln\left(\frac{r_{\rm cool}}{r_{\rm opt}}\right), \qquad (2)$$

where $\dot{M}_{\rm cool}(r_{\rm cool})$ is the rate at which mass is cooling in the dark matter halo and $r_{\rm cool}$ is the cooling radius (which grows with time). This model assumes that the halo has an isothermal potential with circular velocity $V_c$. As shown in the Appendix, the model can be readily extended to the case where the gravitational potential follows the functional form favoured by Navarro, Frenk & White (1996, NFW).

We have used the formulae and parameter choices in the Appendix to predict the bolometric X-ray luminosity for each of the three galaxies, as well as the region in which cooling is expected to occur. Table 5 lists the cooling radii and luminosities of the haloes predicted by WF91's standard model and by a model with an NFW potential. In column 5, we list the luminosity that is expected within the 5-18$'$ annulus used in the observational measurements. This geometric correction is made under the assumption of an isothermal flow in quasi-hydrostatic equilibrium as described in the Appendix. The figure given includes a correction for the flux from the target galaxy that is expected in the outer background annulus by extrapolating beyond the cooling radius with an $r^{-2}$ density profile. The corrected flux is about 50% and 70% of the total for NGC 2841 and NGC 4594 respectively. The larger correction for NGC 2841 arises because the emission from the target almost fills the PSPC field of view. The geometric correction for NGC 5529 is greater because a large proportion of the luminosity is projected onto the optical image of the galaxy. In the case of this galaxy, the large observational uncertainties mean that the emission model is unconstrained.

For both NGC 2841 and NGC 4594 the bolometric X-ray luminosities predicted by the model are strongly inconsistent with the observations. The WF91 model predicts cooling rates of 7.4 and $9.0 M_\odot {\rm yr}^{-1}$ for NGC 2841 and 4594 respectively. Since the mass cooling rate is proportional to the X-ray luminosity in these theories, the simplest interpretation is that the cooling rates in these galaxies are also much less than those predicted by WF91. If we assume that the geometric factors would be unchanged by reducing the cooling rate, we arrive at upper limits to the present-day accretion rate of 0.5 and $1.44 M_\odot {\rm yr}^{-1}$.

Further insight can be gained by considering the total mass of gas within the cooling radius and the mass of the galaxy disk. In the case of NGC 2841 the disk mass can be determined by fitting the galaxy rotation curve. Kent (1987) derives a disk mass of $9.3 \times 10^{10} M_\odot$ allowing a free-fit of disk and isothermal halo parameters. Adopting an NFW model for the halo, Navarro (1998, N98) derives a best-fit disc mass of $5 \times 10^{10} M_\odot$; a significantly smaller disk mass would be inconsistent with the blue luminosity of the disk

(Young et al., 1996). The WF91 model prediction for the mass of gas within $r_{\rm cool}$, which is assumed to have formed the disk, is $9.8 \times 10^{10} M_{\odot}$. Thus the model allows enough gas to cool to make the observed disk. Consequently our data suggest that the present-day accretion rate does not significantly contribute to the total disk mass. Clearly, this is an important result, since (if these galaxies are representative) it implies that the masses of spiral disks have remained almost constant over recent look-back times. Finally, we can compare the gas accretion rate with the star formation rate in NGC 2841 of $0.8 M_{\odot}{\rm yr}^{-1}$ inferred from Ly-$\alpha$ emission (Young et al. 1996). Thus, although the infall rate we find is below that required to build the disk over the Hubble time, the current rate of star formation can almost be maintained by the supply of fresh material.

Before reaching wide ranging conclusions, however, we must ask whether it is possible to modify the emission model to bring it more into line with the observational data. Below we consider possible modifications to the halo model that might reduce the discrepancy with the observational results.

**Cosmological Parameters.** The predicted X-ray luminosities have a relatively weak dependence on the cosmology adopted*. The strongest dependence is on the baryon fraction since the cooling rate is proportional to the square of the density of the X-ray emitting plasma. Using $\Omega_{\rm b} = 0.04$ (a 50% reduction) reduces the luminosities by a factor $\sim 2$, but at the expense of lowering the mass cooling rate also by a factor $\sim 2$. Reasonable changes in cosmological parameters are unable to lower the predicted X-ray luminosity by more than a factor $\sim 3$. In particular, lowering $\Omega_0$ tends to increase the cooling rate and (consequently the X-ray luminosity) because the baryon fraction of the halo is then increased.

**X-ray Emission Temperature.** An assumption of the model is that the X-ray emission occurs at a characteristic temperature close to that of the galactic halo. If the plasma had a multiphase structure, then the emission weighted temperature could be lower. However, a 25% decrease in temperature reduces the expected flux by only 20%. Much larger changes in temperature are required in order to account for the discrepancy.

**Spatial Distribution of X-ray Emission.** Because the cooling radius estimated from NGC 2841 is so large, the correction for the spatial distribution of the X-ray emission is important. For example, in the most extreme case (where we assume that the X-ray emissivity is constant within the cooling radius), the model luminosity (corrected for geometrical effects) would be reduced by a factor of 2 relative to the value given in Table 5. These corrections are much less important for NGC 4594 where the cooling radius is better matched to the PSPC field of view.

**Halo Circular Velocity.** The luminosity of the flow is based on the premise that the high circular velocities of the disks of these galaxies reflect the high circular velocities of the halo that confines the hot plasma. Recently, several authors (Zaritsky et al. 1997, N98) have suggested that high circular velocity galaxies can be formed in significantly cooler haloes. N98 has modelled the rotation curve of NGC 2841. His best fitting model suggests $V_{200} = 167^{+134}_{-13}$ km s$^{-1}$ (where $V_{200}$ is the circular velocity at the virial radius). Using the corresponding potential in the calculation of the X-ray luminosity predicts a substantially reduced X-ray emission of $0.9 \times 10^{41}$ ergs s$^{-1}$ (including geometric factors), in much better agreement with the observational results (ratio to observational upper limit = 0.43).

**Metal abundance.** We have assumed that the hot gas in the haloes has a metal abundance similar to that measured in galaxy clusters, namely $Z = 0.3{\rm Z}_{\odot}$. Using $Z = 0.5{\rm Z}_{\odot}$ increases the predicted X-ray luminosity by approximately 30%, since gas with a higher metal content can cool more efficiently. Reducing the abundance to $0.1{\rm Z}_{\odot}$ would, for the same reason, reduce the predicted luminosities (and gas accretion rates), by a factor of $\approx 3$.

## 4 CONCLUSIONS

We have searched for large-scale diffuse X-ray emission from three nearby, high rotation velocity spiral galaxies. In each case, we find that the observed emission is almost *an order of magnitude* below that required to build the disk at a constant rate within the age of the universe. The accretion rate is similarly discordant with theoretical estimates of the cooling rate of gas in an isothermal or NFW-profile halo.

Although extremely suggestive, our results are not definitive.

- Strong constraints are derived only for two nearby galaxies. We may, by chance, have selected two systems that have anomalous cooling rates. This is plausible for the bulge dominated NGC 4594 galaxy ('the Sombrero'). NGC 2841 appears to be more typical of spiral galaxies, but its proximity makes accurate background subtraction difficult, and our results are dependent on the profile assumed for the X-ray emission. By contrast, the third galaxy meeting our selection criteria is too distant for strong limits on the X-ray flux to be set. We note, however, that the X-ray luminosities detected for these galaxies are compatible with the emission that is thought to occur in the halo of our own galaxy (eg., Moore & Davis, 1994, Wolfire, et al. 1995).
- There are a number of parameters that have been assumed in order to predict the X-ray flux from the properties of the halo. Although no single parameter, can be altered to bring the observations completely into line, these may act together to eliminate the problem. The strongest effect comes from reducing the circular velocity of the halo to considerably below that indicated by the galaxy disk. This has the advantage that it naturally produces both a reduction in the energy released in the flow and a drop in the expected flow rate.

The results, however, encourage further work. The current upper limits are set by our ability to subtract the background count-rate in the images. This is exacerbated in the ROSAT data because the flux level at which individual point sources may be subtracted varies across the image on scales comparable to the spiral galaxy haloes. Future work requires large-scale imaging with a detector that has a near-uniform detection threshold, such as the EPIC camera aboard the

* Unless otherwise stated we have assumed $H_0 = 50$ km s$^{-1}$Mpc$^{-1}$, $\Omega_0 = 1$, $\Lambda_0 = 0$, $\Omega_{\rm b} = 0.06$ and $\sigma_8 = 0.67$

**Table 5.** Predictions from our models, assuming the standard cosmology and halo gas with $Z = 0.3Z_{\odot}$. Columns 3 and 4 list the total model luminosity and cooling radius in arcmin; column 5 gives the model luminosity after correction for the geometry of the source and background annuli; column 6 lists the ratio of the observed luminosity to the model luminosity after correction for the geometry.

| Target | Halo model | Model $L_X/10^{41}$ ergs/s | $R_{cool}$ (arcmin) | Geo. corrected Model $L_X/10^{41}$ ergs/s | Ratio of obs. 95% upper limit to model |
|---|---|---|---|---|---|
| NGC2841 | Isothermal | $10.4 \pm 0.10$ | $35.1 \pm 13.7$ | $5.5 \pm 0.06$ | $< 0.07$ |
| | NFW | $7.6 \pm 0.74$ | $48.0 \pm 18.1$ | $4.5 \pm 0.44$ | $< 0.09$ |
| NGC4594 | Isothermal | $10.8 \pm 0.18$ | $18.7 \pm 1.9$ | $7.6 \pm 0.13$ | $< 0.16$ |
| | NFW | $9.5 \pm 0.63$ | $23.0 \pm 2.4$ | $6.9 \pm 0.46$ | $< 0.17$ |
| NGC5529 | Isothermal | $3.4 \pm 0.03$ | $9.4 \pm 0.4$ | $1.3 \pm 0.01$ | $< 2.9$ |
| | NFW | $2.4 \pm 0.10$ | $12.5 \pm 0.5$ | $0.9 \pm 0.04$ | $< 4.2$ |

XMM satellite (Lumb et al. 1996). Such a survey needs also to target a greater fraction of the nearby galaxies, setting firmer limits on the diffuse X-ray emission and eliminating cosmic variance as a source of uncertainty. If such work continues to fail to make detections, then we would be forced to conclude that spiral disks are no longer growing at the present epoch. This would agree with traditional models of galaxy formation in which galaxies accrete their mass at early times and evolve as more or less closed systems to the present-day. Clearly, there is much to learn from future studies of the X-ray haloes of spiral galaxies.

## ACKNOWLEDGEMENTS

The authors would like to acknowledge Shaun Cole and Julio Navarro for providing rotation curve modelling code and best fit parameters for NGC 2841 respectively. We thank Enzo Branchini for making available to us his peculiar velocity field models prior to publication and Alan Smith for his work on a pilot version of this project as part of his undergraduate studies at the university of Durham. We have made use of the NASA Extragalactic Database (NED) and the Leicester Database and Archive Service (LEDAS). This project was carried out using computing facilities supplied by the Starlink Project, and was supported by a PPARC rolling grant for "Extragalactic Astronomy and Cosmology at Durham" and by the European Community's TMR Network for Galaxy Formation and Evolution. AJB and CSF acknowledge receipt of a PPARC Studentship and Senior Research Fellowship respectively.

## REFERENCES

Abadi, M., Bower, R. G., Navarro, J., 1998, in prep.
Bertschinger, E., 1989, ApJ, 340, 666
Branchini E. et al., 1999, in preparation
Cole, S., Lacey, C., 1993, MNRAS, 262, 627
Cole S. et al., 1994, MNRAS, 271, 781
de Vaucoulers G., 1979, ApJ, 227, 729
Dickey J. M., Lockman F. J., 1990, ARAA, 28, 215
Forman W., Jones C., Tucker W., 1985, ApJ, 293, 102
Young, J. S., Allen, L., Kenny, J. D. P., Lesser, A., Rownd, B., 1996, AJ, 112, 1903
Kauffmann G., White S. D. M., Guideroni B., 1993, MNRAS, 264, 201
Kim D.-W., Fabbiano G., Trinchieri G., 1992, ApJS, 80, 645
Lacey, C., Cole, S., 1993, MNRAS, 262, 627
Lumb, D., Eggel, K., Laine, R., Peacock, A., 1996, SPIE, 2808, 326
Mason et al., 1998, MNRAS (submitted)
Mathews, W. G., Brighenti, F., 1998, preprint, astro-ph/9711103
Moore, B., Davis, M., 1994, MNRAS, 270, 209
Mulchaey, J. S., Davis, D. S., Mushotzky, R., F., Burstein, D., 1996, ApJ, 456, 80
Navarro J. F., 1998, ApJ (submitted) (N98)
Navarro J. F., Frenk C. S., White S. D. M., 1996, ApJ, 462, 563 (NFW)
Ponman T.J. et al., 1994, Nature, 369, 462
Read, A. M., Ponman, T. J., 1998, MNRAS, submitted.
Read, A. M., Ponman, T. J., Strickland, D. K., 1997, MNRAS, 286, 626
Snowden, S.L., McCammon, D., Burrows, D.N., Mendenhall, J.A., 1994, ApJ, 424, 714
Trinchieri G., Kim D. W., Fabbiano G., 1994, ApJ., 428, 555
Trinchieri G., Fabbiano G., Kim D. W., 1997, A&A, 318, 361
Tully R. B., Fouqué P., 1985, ApJS, 58, 67
White S. D. M., Frenk C. S., 1991, ApJ, 379, 52 (WF91)
Wolfire, M. G., Mckee, C. F., Hollenbach, D., Tielens, A. G. G. M., 1995, ApJ, 453, 673
Zaritsky D., Smith R., Frenk C. S., White S. D. M., 1997, ApJ, 487, 39

## APPENDIX A: A SIMPLE MODEL FOR THE X-RAY EMISSION FROM COOLING GAS

Following WF91, we assume that cooling occurs within a static potential, and that the cooling gas remains isothermal as it flows to the centre. The assumption of isothermality allows considerable simplification in the determination of the X-ray luminosity of the flow since it is directly related to the drop in potential energy (ie., the internal energy of the gas remains constant). Detailed, fully self-consistent flow models, such as those of Bertschinger (1989) and Abadi et al (1998), show that these assumptions are reasonable over the range of scales over which we wish to determine the flow solution. The X-ray luminosity emitted by a unit mass of gas as it moves within the potential, $\phi$, is

$$l_X = -v_R \frac{\partial \phi}{\partial r}. \qquad \text{(A1)}$$

We find the total energy emitted by this component of gas as it flows inwards and then integrate from $r_{cool}$ to $r_{optical}$ to find the total energy emitted by the mass of gas,

$$q = \int_{r_{\rm optical}}^{r_{\rm cool}} -\frac{l_{\rm X}(r)}{v_{\rm R}(r)} {\rm d}r. \quad \text{(A2)}$$

If we now make the assumption that mass flows to the centre more quickly than the structure of the flow changes, then the structure of the flow at a snapshot in time can be represented by the trajectory of a single mass unit. Hence

$$L_{\rm X} = \dot{M}_{\rm cool}(r_{\rm cool}) \int_{r_{\rm optical}}^{r_{\rm cool}} \frac{V_{\rm c}^2(r)}{r} {\rm d}r. \quad \text{(A3)}$$

Below we consider two possibilities for the structure of the dark matter halo. In §A1 we consider an isothermal halo and in §A2 we consider the dark matter profile described by NFW, in each case assuming that the gas initially traces the dark matter.

### A1 Cooling in an Isothermal Halo

This potential was considered by WF91. The dark matter density profile is $\rho(r) \propto r^{-2}$, where $r$ is radial distance in the halo. The cooling radius, $r_{\rm cool}$, in the halo is defined as the radius at which the cooling time, $t_{\rm cool}$, of the gas equals the age of the Universe, $t_0$. Ideally, we would use the time since the halo last doubled in mass (Cole & Lacey, 1993), but this information is not available for an individual galaxy. Since mass cooling rates decline with time, this leads to a conservative comparison with our observational results.

Assuming a spherically symmetric halo in which the gas is initially distributed like the dark matter, the cooling time is given by

$$t_{\rm cool}(r) = \frac{192\pi\Omega_0 {\rm G m_p^2} r^2}{49 f_{\rm g} \Omega_{\rm b} \Lambda(\mu {\rm m_p} V_{\rm c}^2/2{\rm k})}, \quad \text{(A4)}$$

(White & Frenk 1991), where $\Omega_{\rm b}$ is the baryon fraction, $\Lambda(T)$ is the cooling function of the gas, $f_{\rm g}$ is the fraction of the initial baryon density remaining in gaseous form, G is the gravitational constant, $\rm m_p$ is the mass of a proton, $\mu$ is the mean molecular weight of the gas, $V_{\rm c}$ is the circular velocity of the halo and k is Boltzmann's constant.

The evolution of the cooling radius determines the mass of gas cooling per unit time.

$$\dot{M}_{\rm cool}(r_{\rm cool}) = \frac{1}{2} \frac{f_{\rm g}\Omega_{\rm b}}{\Omega_0} \frac{V_{\rm c}^2(r_{\rm cool}) r_{\rm cool}(V_{\rm c,max}, z)}{{\rm G} t_0}. \quad \text{(A5)}$$

This can be combined with equation (A3) to estimate the total X-ray luminosity of the halo.

### A2 Cooling in an NFW Halo

NFW provide a fitting formula for the density profiles of dark matter haloes in N-body simulations of hierarchical clustering. This profile is characterised by two parameters: $\delta_c$, a characteristic density, and $r_s$, a characteristic radial scale in the halo. NFW find that $\delta_c$ and $r_s$ are correlated in any given cosmology so that the NFW profile provides a universal, one-parameter model of the halo. This formula provides a good approximation to the density profile of haloes of all masses over at least two orders of magnitude in radius and its shape is independent of the values of the cosmological parameters.

Appropriate parameters for the galaxy haloes in any given cosmology are determined by requiring that the measured circular velocity of the galaxy corresponds to the maximum in the NFW rotation curve. This must be fitted in an iterative fashion since the ratio between $V_{\rm c,vir}$ and $V_{\rm c,max}$ itself depends on $c = r_{200}/r_s$.

Using the circular velocity profile of an NFW halo, the cooling radius is defined by the relation

$$\begin{aligned} t_0 &= \frac{192\pi}{49} \frac{1}{f_{\rm g}} \frac{\Omega_0}{\Omega_{\rm b}} \frac{{\rm Gm_p^2} r_s^2}{\Lambda(T_{\rm vir})} \frac{x_{\rm cool}}{x_{\rm vir}} (1 + c x_{\rm cool})^2 \\ &\times [\ln(1 + c x_{\rm vir}) - c x_{\rm vir}/(1 + c x_{\rm vir})]^{-1}. \end{aligned} \quad \text{(A6)}$$

where $x = r/r_{200}$. We then obtain,

$$\begin{aligned} L_{\rm X} &= \dot{M}_{\rm cool}(r_{\rm cool}) V_{\rm c}^2(r_{200}) \\ &\times \int_{x_{\rm optical}}^{x_{\rm cool}} x^{-2} \frac{\ln(1+cx) - cx/(1+cx)}{\ln(1+c) - c/(1+c)} dx, \end{aligned} \quad \text{(A7)}$$

where $x_{\rm cool} = r_{\rm cool}/r_{200}$ and $x_{\rm optical} = r_{\rm optical}/r_{200}$. This equation must be integrated numerically for any given $c$.